Fault Detection and Isolation of a Wind Turbine

Alexandru Cohal, Letiția Mirea

Faculty of Automatic Control and Computer Engineering
"Gheorghe Asachi" Technical University of Iași, Romania
(e-mail: cohal.alexandru@ac.tuiasi.ro, lmirea@ac.tuiasi.ro)

Abstract: In this paper, several methods used for detection and isolation of different types of faults which can affect a wind turbine are presented. These methods can be divided into two categories: model-based methods (designing a state-space estimator is considered) and methods based on the wind turbine's signals analysis (in both frequency and time domains). A benchmark model implemented in Matlab and Simulink of a real wind turbine (Odgaard, et al., 2009) is used to test these fault detection and isolation methods. The faults considered in this model affect some of the sensors and the actuators of the wind turbine. The developed methods are implemented as Simulink blocks and placed in the wind turbine's benchmark model, allowing an online detection and isolation of the considered faults. The obtained results are then analysed.

Keywords: Fault Detection and Isolation, Wind Turbine, Analytical Model, Spectral Analysis, Statistical Analysis.

1. INTRODUCTION

The need for energy and especially for electrical energy has increased impressively in the last century. According to (Sathyajith, 2006), the growth rate of energy consumption over a year is 3.2% for developing countries (due to the population increase and the development of technologies) and 1.5% for industrialized countries.

Nowadays, the most energy is produced using non-renewable resources: coals, natural gases and oil. The disadvantages implied by the usage of these resources (excessive pollution level, high extraction and transportation costs, exposure to various hazards, almost total consumption of these resources) have determined a change towards usage of renewable resources in recent years.

Thus, the interest in wind power has increased due to its advantages, leading to numerous research works, governmental agreements and construction of numerous wind turbines of different sizes and powers all over the world. The advantages of wind power are: reduced production costs of electrical energy, reduced construction time of the systems which use this type of energy to produce electricity (wind turbines), the global availability and the absence of any usage costs of this resource, the dependence on countries rich in oil and natural gases is eliminated and also, devastating accidents (as in the case of nuclear plants) cannot occur anymore (Mukund, 1999; Chiras, 2010). On the other hand, the wind power has some disadvantages too: the winds have a variable behaviour in time - over several years (a long-term prediction can be made after acquiring information during 30 years), over a year (the wind power varies depending on the season: usually, during winter and autumn the winds are stronger), over a day (diurnal changes) and short-term variations (turbulences, gusts), (Manwell, et al., 2009). Thus, a wind turbine produces electrical energy over 65% - 80% of a year and generates the maximum power only on 10% of the operating time. There are also some other disadvantages, but their effects are less important: the level of noise produced by a wind turbine during the operating time is similar with the noise of a running refrigerator (55 dB), interference of wind turbines with radio and television signals, the wind turbines are responsible for the death of less than one bird for each 10.000 birds killed by human activities and the effect of the wind turbines on the natural environment is very reduced because these systems are usually built in those areas where power lines which had modified the environment already exist (Chiras, 2010; American Wind Energy Association, n.d.). The electrical power developed by a wind turbine has increased impressively from 50 kW in 1985 up to 10 MW in 2015 at the same time with the dimension (the rotor diameter increased from 15 meters up to 190 meters). The price of the electrical power produced experienced a dramatic fall between 55 cents in 1980 and 4 cents in 2014 for a kWh (ABB, 2011; American Wind Energy Association, 2014).

The rising popularity of wind turbines due to their advantages has determined an increase in the study of maintenance solutions for these systems. The repair and maintenance costs represent a significant part of the operating price of a wind turbine. The offshore placement of the wind turbines implies higher costs than the onshore placement. Thus, various types of systems which detect and isolate the faults which may occur during the operation of a wind turbine have been developed over the years. The reasons of designing very effective such systems are that an early and prompt detection of a fault can extend the lifetime of the wind turbine, reduce the repair costs and can determine a change of its operating parameters to avoid the total shutdown of the turbine, even if its operation is not optimal (Ozdemir, et al., 2011; Tabatabaeipour, et al., 2012).

The subject of fault detection and isolation for a wind turbine has been considered in various papers. A review of some of these articles is made in (Odgaard and Stoustrup, 2012). Other contributions in this field are: (Wenxian and Tavner, 2008; Esbensen and Sloth, 2009; Wenxiu and Fulei, 2010; Hajiabady, et al., 2014). Some other papers presenting fault detection and isolation methods which can be also applied also for the case of a wind turbine are: (Venkatasubramanian, et al., 2003; Mendes, et al., 2006; Lee, 2008; Poulsen and Niemann, 2009).

In this paper, different types of faults which can affect a wind turbine are studied and methods of detecting them are then provided. These methods are tested using a benchmark model of a wind turbine (Odgaard et al., 2009) implemented in Matlab and Simulink. In order to do this, the Fault Detection and Isolation (FDI) methods are designed for operating in real-time and implemented as Simulink blocks.

The paper is organized as follows: Sections 2 briefly presents the components and the operation of a wind turbine. In Section 3 it is presented and explained the wind turbine's benchmark model implemented in Simulink (Odgaard, et al., 2009) which is used in this paper for testing the FDI methods. Section 4 contains the description of the applied FDI methods. The obtained results are detailed in Section 5. Finally, the conclusions are given in Section 6.

2. COMPONENTS AND OPERATION OF A WIND TURBINE

To transform the kinetical energy of the winds into mechanical energy and then into electrical energy, various solutions have been developed. The main criterion to classify these solutions is the type of rotor's axis. Thus, the wind turbines can have vertical or horizontal axis. Because the vertical axis wind turbines can use winds from any direction, their construction is simpler (it is not needed a yaw rotational system like in the case of horizontal axis wind turbines; the gearbox and the generator are placed on the ground, not inside the nacelle). So, the maintenance operations are easier to perform. Although, this type of wind turbine has some major drawbacks: a starting system is required because exists some aerodynamically dead-zones from which the turbine cannot start on its own, reducing at the same time the efficiency of the system. A precise control of the wind turbine is required because a strong wind may determine the blades to spin at a very high speed (Sathyajith, 2006).

Most of the wind turbines used nowadays have horizontal axis due to their advantages: low cut-in wind speed and easy furling. They have mechanisms that can adjust the yaw angle of the nacelle and the pitch angles of the blades in order to control the outputted electrical power and to protect the construction from strong winds. The need of having these mechanisms together with the position of the gearbox and the generator in the nacelle implies a more complex and expensive design of the wind turbine (Sathyajith, 2006).

The horizontal axis wind turbines can be classified according to: number of blades (single bladed, two bladed, three bladed or multi bladed), direction of receiving the wind (up-wind or down-wind), number of rotors (single or multiple), position of the wind turbine (onshore or offshore) and quantity of produced power (low, medium or high).

Further on, the paper will be focused on wind turbines having horizontal axis, three blades and a single rotor facing the wind directly (up-wind).

A wind turbine consists of three main components: a tower, a nacelle and a rotor. The main purposes of the tower is to support the nacelle and the turbine at the optimum height obtained after the design process and to sustain the entire structure unaffected by the vibrations caused by the variations of wind speed. The wind contains less turbulences at high altitudes so higher towers are preferred. However, a very high tower implies the occurrence of stability issues (Khaligh and Onar, 2010). For a high power wind turbine, the tower is usually tubular (made of concrete or steel) or latticed. For a low power wind turbine, the tower can be sustained by cables (Mukund, 1999). According to the type of used tower and the soil in which the turbine is constructed, different foundations can be used (e.g. slab, mono-pile and multi-pile) (Burton, et al., 2001).

The rotor is the most important and prominent component of a wind turbine. It transforms the kinetic energy received from the winds into mechanical rotational energy. This energy is applied to the shaft connected with the rotor (Wagner and Mathur, 2009). This shaft, together with the blades and the hub, are the main components of the rotor.

Blades of a wind turbine and wings of an airplane have the same basic principles of working. Because the wind turbines work in a different environment (which implies often changings of wind speed and wind direction), certain details are considered in their design process in particular (Wagner and Mathur, 2009). Blades of the modern wind turbines are made with aerofoil sections (one half of the blade is rounded, whereas the other half is almost flat). Thus, areas with different pressures are formed above and below the blade according to Bernoulli's theorem. The difference between the pressures implies the appearance of a force which rotates the rotor. Different characteristics of the blades are chosen (e.g. type of material, length, and lightning protection) according to the desired performances of the wind turbine (Sathyajith, 2006).

In order to control the output power, some wind turbines (named pitch controlled wind turbines) have mechanisms inside the hub for rotating the blades around their pitch axis. The turbine's controller checks the values of the generated power using a certain sampling period. When this power is higher than a threshold value, a signal is sent to the blade pitch mechanism which turns the rotor blades out of the wind. Contrary, when the generated power is too low, the blades are turned back into the wind (Wagner and Mathur, 2009). Also, this pitch system is useful in case of an emergency situation. By rotating the blades such that the aerodynamic forces are at the lowest values and activating simultaneously the breaks, the rotation of the rotor can be stopped much faster. These systems have an energy accumulator in order to continue to work for a short time if the energy supply is interrupted (Gasch and Twele, 2012).

The blades are connected one to each other through a hub. This is one of the critical components of the rotor because requires a proper design and has to be built from a suitable material in order to ensure high strength qualities (Sathyajith, 2006). The spinner is a capsule which covers the hub, has an aerodynamic shape and protects the hub and the pitch systems against bad weather effects (rain drops, snow, dust).

Usually, the components of the drive train and those of the electrical system are enclosed in a nacelle (Fig. 1) which can be connected with the tower through a rotational mechanism (called yaw system) or through a fixed joint. The drive train includes all the rotating parts of a wind turbine and those components which assure them the proper functionality: hub, shafts, gearbox, clutch and bearings. All these components form a functional unit and have to be considered always together (Hau, 2013). The rotor is connected through the hub with the low-speed shaft which transmits the rotational energy to the gearbox. This component transforms the rotational speed of the rotor to the speed required by the generator and delivers it through the high-speed shaft (Gasch and Twele, 2012). The generator converts the rotational speed to electric energy which is then adapted to the required voltage and frequency of the electrical grid through a transformer and two inverters (AC-DC and DC-AC) (Wagner and Mathur, 2009; Hau, 2013).

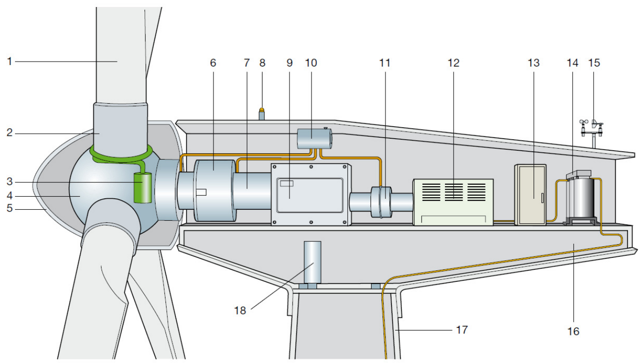

Fig. 1. The main components of a horizontal axis wind turbine (1 – blade, 2 – blade support, 3 – pitch angle actuator, 4 – hub, 5 – spinner, 6 – low-speed shaft support, 7 – low-speed shaft, 8 – safety lights, 9 – gearbox, 10 – mechanical breaks, 11 – hydraulic cooling device, 12 – generator, 13 – inverters, controller and protection device, 14 – transformer, 15 – anemometer, 16 – frame of the nacelle, 17 – tower, 18 – yaw driving device) (ABB, 2011).

Besides the components of the drive train and the electric system, there are also secondary components inside the nacelle (Fig. 1) which have important roles: cooling, heating, lubricating, breaking, data acquisition, maintenance, alarming and safety-signalizing (Hau, 2013).

The main purpose of the control system of a wind turbine is to allow it to function completely autonomous. Moreover, the wind turbine has to function in a safe manner in any conditions without affecting itself or the environment. In order to do this, the possible faults which can occur have to be detected or predicted and specific measures have to be taken (Hau, 2013). Thus, the control system is composed of dynamic subsystems (manages the operation of the wind turbine, establishing reference values for the blade pitch angles, nacelle's yaw angle and output power according to the current conditions) and supervisory subsystems (monitors the operation of the wind turbine and takes appropriate measures (e.g. start, shut-down, breaking and accommodate faulty sensors) (Manwell, et al., 2009).

3. THE MODEL OF A WIND TURBINE

A benchmark model of a wind turbine was developed in Matlab and Simulink (Odgaard, et al., 2009) and will be used in this paper to test the fault detection and isolation implemented methods.

According to (Odgaard, et al., 2009), the considered benchmark model corresponds to a real wind turbine, characterized by horizontal axis and single up-wind three-bladed rotor. It can function with variable speed winds due to its pitch systems, even though the yaw system is absent. The rated power is 4.8 MW and is obtained by using a generator fully coupled to a converter.

The main components of a wind turbine are modeled in four different blocks in the benchmark model. The Blade and Pitch Model describes the hydraulic rotational system of the blades and the aerodynamic effects of the wind on the blades depending on the pitch angles. The Drive Train Model is used to describe the mechanical behaviour of the components which connect the rotor and the generator. The functioning of the generator that produces electrical energy from mechanical energy is modeled in the Generator and Converter Model, together with the operation of the converter which modifies the torque. The control of the modelled wind turbine is performed in two stages: power optimization (when the wind speed is too low to obtain the desired electrical power, optimization tehniques are applied in order to obtain the highest possible power level) and power reference follow (pitch angles of the blades are modified by a PI controller in order to maintain the desired output power when the wind speed is strong enough) (Odgaard, et al., 2009).

These blocks and the connections between them are shown in Fig. 2. In order to follow the imposed electrical power reference (P_r) and to minimize the difference between this power and the actual generated power (P_g), the controller of the wind turbine has to generate reference values for the pitch angles of the blades (β_r) and for the generator's torque ($\tau_{g,r}$) based on the measured values (β_m, $\tau_{g,m}$). These reference values are transmitted to the Blade and Pitch System Block (β_r) and to the Generator and Converter Block, respectively ($\tau_{g,r}$). The pitch systems modifies the blade's angles according to the reference value received. Based on the values of the wind speed (v_w) and the aerodynamic forces that are influenced by the pitch angles of the blades, a different value of the rotor's torque (τ_r) is generated. This torque is applied to the wind turbine's Drive Train which influences the rotational speed of the rotor's shaft (ω_r) and the rotational speed of the generator's shaft (ω_g). Based on the last rotational speed (ω_g) and on the reference for the generator's torque ($\tau_{g,r}$), the generator produces a certain torque value (τ_g) and electrical power (P_g).This represents the produced electrical power by the wind turbine.

The benchmark model implemented in Matlab and Simulink has two more blocks than the diagram in Fig. 2: the Wind Model's block and the Sensors' block. The sensors considered in the benchmark model have been grouped in a separate block in order to simplify the model. Aiming to simulate the real behaviour of the sensors, stochastic noise overlaps the real measured values. Physical redundancy is assured by the usage of two sensors for each measured property: pitch angle of each blade (β), rotor's rotational speed (ω_r), generator's rotational speed (ω_g) and rotor's torque (τ_r). Only one sensor was considered for generator's torque (τ_g), electrical power obtained (P_g) and wind speed (v_{hub}). Based on a predefined real measurements sequence of wind speed obtained from a wind park, the behaviour of the wind is simulated in the Wind Model block. Inside this block, the phenomena which occur in real situations are simulated: wind shear (variation of the wind speed over altitude), tower shadow (changing of the wind direction because of the wind turbine's tower) and turbulences (simulated using a Kaimal filter). Thus, the wind speed at the hub level (v_{hub}) and at blades level (v_{wind}) are obtained as outputs of this block.

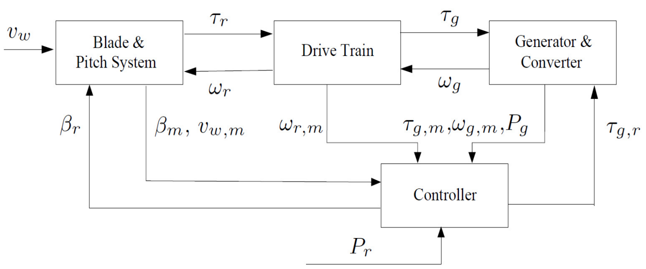

Fig. 2. The block-diagram of the considered benchmark model (Odgaard, et al., 2009).

During the simulation of the benchmark model, nine faults are introduced at different time moments. These faults affect three types of components: sensors (5), actuators (3) and drive train (1). The faults have different degrees of severity and in consequence, different counter-actions have to be taken after detection and isolation. Some faults are very serious and should determine the shutdown of the entire system, whereas some are less severe and the controller can accommodate the resulted effects (Odgaard, et al., 2009).

This paper is focused only on three types of faults which affect the sensors and an actuator simulated in the benchmark model and further on, only these faults will be detailed.

4. FAULT DETECTION AND ISOLATION

A fault is a phenomenon which leads to a change in the behaviour of a system such that the performances imposed for a particular functionality are not fulfilled anymore. So, the system will continue to function, but not in the optimal designed manner. In contrast, a failure makes the system to not be able to fulfil a designed functionality. In this case, the shut-down of the system is required (Marcu and Mirea, 2003; Blanke, et al., 2006).

Although faults, perturbations and modelling uncertainties cause changes in the normal operation of a system, there are some differences between them. The effects of a fault have to be detected and counteracted as fast as possible because sudden or gradual unknown changes will appear (Marcu and Mirea, 2003). These differences cannot be reduced by a classical controller. In contrast, the effects of perturbations and modelling uncertainties are known and can be withstood by using filtering methods or adaptive control (Blanke, et al., 2006).

The occurrence of a fault implies not only a change in the behaviour of the affected component, but also in the entire ensemble which includes that part. In order to avoid the damaging of the system, of the connected elements or of the environment, the faults have to be detected as fast as possible and decisions have to be taken in order to restrict the effects. Thus, a fault tolerant control has to be implemented. The functionalities of the system will be fulfilled even when a fault occurs by the self-adaptation of the controller to the new structure or parameters of the system (Blanke, et al., 2006).

A fault tolerant system has two stages: fault diagnosis (the fault and its source has to be detected) and adaptation of control law (modification of controller's parameters in order to counteract the effects of the fault). The first stage implies four steps: detection (finding the moment when a fault appears), isolation (finding the component affected by the fault), identification (finding the type of the fault) and estimation (finding the severity level of the fault). This paper is focused only on the first two steps of the fault diagnosis process.

The wind energy is the renewable energy with the highest annual increase. According to (Global Wind Energy Council, 2015), only in the year 2014, wind turbines with a cumulated power of 51 GW were installed. Simultaneously with the development of the maximum power delivered, protection and maintenance solutions were also improved. For both onshore and offshore wind turbines, the use of a fault tolerant controller offers multiple advantages: production of electrical energy in small quantities even when a fault occurs, protection of the system, less frequent and less expensive maintenance operations and increase of profit (Esbensen and Sloth, 2009). Thus, every wind turbine should have a supervising system in order to monitor the components and to detect the faults. The most frequent faults in a wind turbine affect sensors, actuators, drive train and electrical system (Manwell, et al., 2009).

Regarding the usage of an analytical model, fault detection methods can be divided in two categories. The detection can be based on *a priori* knowledge about the model of the studied component or can be done empirically, using the *black-box* concept. Even though both methods use models and data acquired from the system, the manners which yield to the results are completely different (Katipamula and Brambley, 2005).

4.1. Fault Diagnosis based on Analytical Model

Using *a priori* knowledge (physical equations) about the component which is diagnosed, a model is designed such that its behaviour is the same as the real one in normal conditions (without faults). This model has the same inputs as the real component. Comparing the outputs of the system and of the model, respectively, a residue is obtained. By analysing this residue using different techniques, it can be established if a fault occurred or not. This method of fault detection has the advantage of underlying on physical principles which describes the behaviour of the analysed component, but not always a complete model can be obtained (Katipamula and Brambley, 2005).

In the case of the studied wind turbine, a residues generator is designed using a state-space estimator. Thus, the error of the output's estimation can be used as a residue in order to detect the presence of a fault. It is considered the linear, time-invariant, observable model in state-space representation of the analysed component in normal behaviour described by the relations (1) and (2) (where $x \in \mathbb{R}^{n\times 1}$ is the state vector, $u \in \mathbb{R}^{m\times 1}$ is the input vector, $y \in \mathbb{R}^{p\times 1}$ is the output vector, $A \in \mathbb{R}^{n\times m}$ is the system matrix, $B \in \mathbb{R}^{n\times m}$ is the input matrix and $C \in \mathbb{R}^{p\times n}$ is the output matrix). The equations of the state-space estimator are (3) and (4) (where $L \in \mathbb{R}^{n\times p}$ is the estimator's matrix, $\hat{x} \in \mathbb{R}^{n\times 1}$ is the estimated state vector and $\hat{y} \in \mathbb{R}^{n\times 1}$ is the estimated output vector). The estimator's matrix L is chosen such that its dynamic is faster than the system's (Luenberger, 1966; Marcu and Mirea, 2003; Radisavljevic-Gajic, 2014). The difference between the real output and the estimated output represents the residue used for fault detection.

$$\dot{x}(t) = A \cdot x(t) + B \cdot u(t) \tag{1}$$

$$y(t) = C \cdot x(t) \tag{2}$$

$$\dot{\hat{x}}(t) = (A - L \cdot C) \cdot \hat{x}(t) + B \cdot u(t) + L \cdot y(t) \tag{3}$$

$$\hat{y}(t) = C \cdot \hat{x}(t) \tag{4}$$

In the case of the modelled wind turbine, a stochastic noise affects the outputs because these are available through sensors' measurements. In order to have the residue influenced only by the faults, a low-pass Butterworth filter has to be used to reduce the effects of the noise. The reason of choosing a Butterworth filter is that its pass-band is flat (no ripples are present). Thus, the important frequencies of the signal will not be distorted, otherwise, the specific frequencies for a certain type of fault could have been covered or even introduced (Proakis and Manolakis, 1996; Pollock, 1999).

The block scheme of the fault diagnosis module based on analytical model used in the case of the wind turbine is showed in Fig. 3.

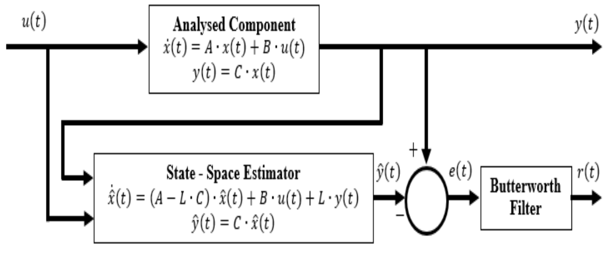

Fig. 3. The block scheme of the fault diagnosis module based on analytical model.

4.2. Fault Diagnosis based on Direct Processing of the Signals

A priori knowledge is not used in this method, contrary to the previous one, only input and output signals of the analysed component. This method also constructs a model which is based only on the behaviour of the component, not on the physical relations (Katipamula and Brambley, 2005).

The methods in this category can be divided in two main classes: those based on frequency-domain analysis and those based on time-domain analysis.

4.2.1. Frequency-Domain Analysis

This method uses *Fourier Transform (FT)* to obtain information about its frequency spectrum through the magnitude and the phase of the sinusoids that comprise the analysed signal.

A reduction of the number of operation required to obtain the frequency spectrum can be made using the *Fast Fourier Transform (FFT)* which is based on the 'Radix-2 decimation-in-time' algorithm firstly described in (Cooley and Tukey, 1965). If the initial analysed sequence is divided in two equal parts, the *Discrete Fourier Transform (DFT)* is applied for each of them and then the results are combined using relation (5), the same result as applying *DFT* for the entire sequence is obtained. Using the symmetry (6) and periodicity (7) properties, a reduction to half of the number of computational operations is obtained because the terms $G(k)$ and $W_n^k \cdot H(k)$ can be used twice, for both $X(k)$ and $X\left(k + \frac{N}{2}\right)$ (relations (8) and (9)) (Dahnoun, 2000).

$$X(k) = G(k) + W_N^k \cdot H(k), where\ k = 0, \dots, N-1 \tag{5}$$

$$W_N^{k+\frac{N}{2}} = -W_N^k \tag{6}$$

$$W_{\frac{N}{2}}^{k+\frac{N}{2}} = W_{\frac{N}{2}}^k \tag{7}$$

$$X(k) = G(k) + W_N^k \cdot H(k), where\ k = 0, \dots, \frac{N}{2} - 1 \tag{8}$$

$$X\left(k + \frac{N}{2}\right) = G(k) - W_N^k \cdot H(k), where\ k = 0, \dots, \frac{N}{2} - 1 \tag{9}$$

Thus, it is recommended that the sequence which is analysed to have a length equal with a power of two in order to reduce the number of computational operations using the *Divide and Conquer* method. Otherwise, zeros will have to be added at the end until a proper length is reached.

Because the diagnosis is made online, the signal processing using FFT has to be performed over temporal windows. The length of the windows has to be chosen such that: sufficient information is enclosed for a precise analysis (all the frequencies involved can be detected if the window's length is bigger than half of the maximum period of the sinusoidal components), the computational time required to process these data do not exceeds the acquisition period of the next sequence and an eventual fault has to be signalized as soon as possible.

The usage of temporal windows has the disadvantage of implying the 'leakage' phenomenon (in spectral representation, some frequencies can be covered by smaller lobes which appear around the principal frequencies' lobes). This problem can be overtaken using a window with a *Discrete Time Fourier Transform (DTFT)* close as possible to a Dirac impulse (Lang, 2014), instead of a rectangular window. The most used such windows are *Hanning* and *Hamming*.

These windows have the disadvantage of attenuating the signal around its ends. Thus, the windows have to be overlapped with a certain percent, such that all the values of the signal can contribute equally to the final result of the analysis. Using this method, the diagnosis system does not have to acquire a set of data equal with the length of the window in order to analyse if a fault is present or not. A shorter sequence of values is required now, which is concatenated with a part of the previous sequence. Thus, the diagnostics can be given faster, fulfilling one of the requirements of a performant diagnosis system – the promptitude (Marcu and Mirea, 2003).

4.2.2. Time-Domain Analysis

The methods from this category use the signals without transforming it into another domain. Four techniques were used in the case of the wind turbine's fault diagnosis: mean (used to detect a continuous component of the signal), dispersion (used to detect the spread of the signal's values around the mean value), auto-correlation (used to detect any repetitive sequence in the signal) and cross-correlation (used to detect the similarity between the signals from the sensors which ensure physical redundancy).

5. IMPLEMENTATION

In order to simulate the behaviour of the wind turbine in conditions as close as possible to the real case, a predefined measurements sequence of wind speed acquired from a real wind park is used. As described in Section 3, this sequence is modified by simulating the phenomena of wind shear, tower shadow and turbulences. After that, the values are used as inputs in the model of the wind turbine. The duration of the wind speed measurement sequence is 4400 seconds, having a sample time of 0.01 seconds.

In this paper, only the detection and isolation steps are analysed, within the diagnosis stage of a wind turbine. Amongst all the faults simulated in this model, in this paper are studied only five of them which can be grouped in three categories: fixed value faults in sensors, gain factor faults in sensors and offset value faults in actuators. Further on, for each fault will be detailed the following: the effects, the severity level, the methods used for detection, the condition which has to be used in order to implement automatic detection and the implementation of the detection block built in Simulink. The results and the performances obtained are detailed and discussed in the next section, together with the isolation problem.

5.1. Fixed value faults in sensors

In the considered model of a wind turbine, three faults affect the sensors by modifying their outputs to constant values, indifferent of the values measured:

- *Fault_1* – blocks the first sensor of the pitch angle of the first blade ($\beta_{1,m1}$) to the value 5° in the time interval $[2000, 2100]\ s$ (Fig. 4)
- *Fault_3* – blocks the first sensor of the pitch angle of the third blade ($\beta_{3,m1}$) to the value 10° in the time interval $[2600, 2700]\ s$
- *Fault_4* – blocks the first sensor of the angular velocity of the rotor ($\omega_{r,m1}$) to the value 1.4 $\frac{rad}{s}$ in the time interval $[1500, 1600]\ s$.

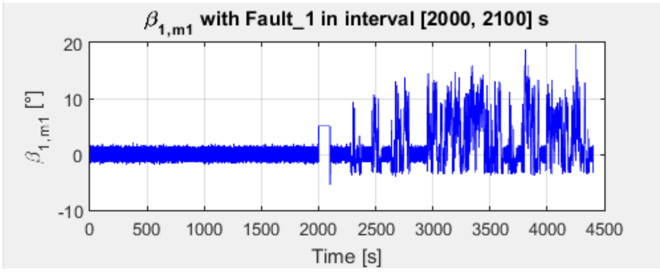

Fig. 4. Pitch angle of the first blade measurements made by the first sensor ($\beta_{1,m1}$) affected by the fixed value fault *Fault_1* in the time interval $[2000, 2100]\ s$.

These faults imply an incorrect measurement which affects the control loops due to the erroneous feedback received by the controllers from the system. Thus, the level of the generated power is affected, but more dangerous effects can appear, like overloading the actuating mechanism of a blade's pitch angle.

The severity of these faults is considered to be reduced, due to the fact that physical redundancy is assured by using two sensors to measure the same physical phenomenon. Thus, a counteract action can be taken in this case, the entire shut-down of the system being unnecessary.

The two methods used to detect these faults are based on mean computation and frequency spectrum analysis.

By computing the mean of the output values of a sensor over temporal windows, consecutive equal values will be obtained in the case of the occurrence of this type of fault. Even the measured feature (e.g. pitch angle) does not change over a period of time, due to the stochastic noise which affects the sensor, different values will be obtained at the output. The sensors provide values having four digits after the decimal point, ensuring a very large set of possible values. Thus, the probability that two or more consecutive means computed over temporal windows during normal operation to have the same value is very low. Good results with respect to fault detection based on this method gave been obtained by verifying the mean values obtained over the last three temporal windows, each one containing 5 samples without any overlapping. The results of computing the mean in the case of $\beta_{1,m1}$ signal affected by the *Fault_1* are presented in Fig. 5.

In the frequency spectrum of the sensor's output, the dominant frequency is $0\,Hz$ only if a fixed value fault is present. When this type of fault occurs, the output of the analysed sensor is constant, without having any oscillation. Thus, the signal can be represented as a single sinusoid having the $0\,Hz$ frequency and the amplitude equal with the fixed value from the output. As described in Section 4, the frequency spectrum will be determined using temporal windows. If the sum of the frequencies' amplitudes except the first frequency (corresponding to the $0\,Hz$ frequency) and the next few (which determines the lobe centered on the $0\,Hz$ frequency) is smaller than a small threshold value, then the fixed value fault is considered to affect the analyzed sensor. Using a temporal window of 512 samples, an overlapping factor of 75% (in order to obtain fast results of the detection and to leave enough time to process all the values acquired), *Hanning* type windows and a threshold value of 0.01. The results of computing the frequency spectrum in the case of $\beta_{1,m1}$ signal affected by the *Fault_1* are presented in Fig. 6.

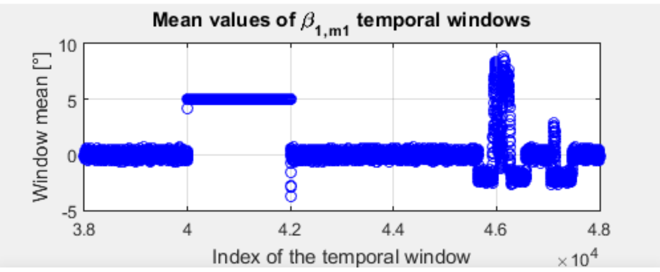

Fig. 5. Mean values of the temporal windows containing 5 samples of $\beta_{1,m1}$ signal. It can be observed that when the fixed value fault *Fault_1* is present, the mean values are equal with the constant output value of the sensor.

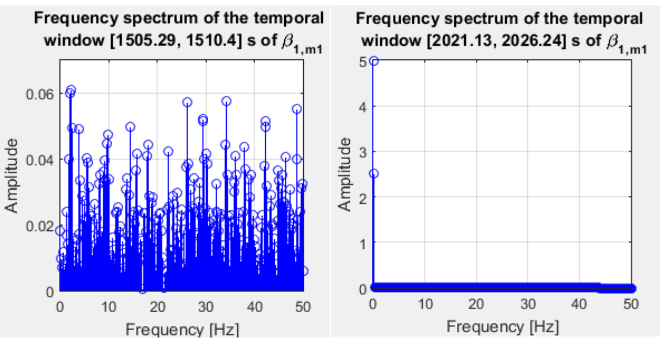

Fig. 6. Frequency spectrums of the temporal windows $[1505.29, 1510.4]\,s$ and $[2021.13, 2026.24]\,s$ respectively, computed over 512 samples using a *Hanning* type window. It can be observed that the $0\,Hz$ frequency is the main one when the fixed value fault *Fault_1* is present.

In order to reduce the probability of a wrong detection of this type of fault, the results delivered by these two methods can be used together. The fault is considered to be present if both methods' conditions are fulfilled and not to be present if both methods' conditions are not fulfilled. If just only one method indicate that the fault is present, then an uncertainty state is considered (when the counteract actions can be prepared but not applied yet).

The structure of the Simulink block which applies the presented methods of detection a fixed value fault (*Fault_1*) in a sensor is presented in Fig. 7. Only the block which detects the first fault (*Fault_1*) will be detailed further on because the other two blocks are similar. This block has as input the analysed signal from the sensor, in this case the measurement of the pitch angle of the first blade ($\beta_{1,m1}$) and as output a signal which can have only three values: 0 if the fault is absent, 2 if the fault is present and 1 if it the uncertainty state is present.

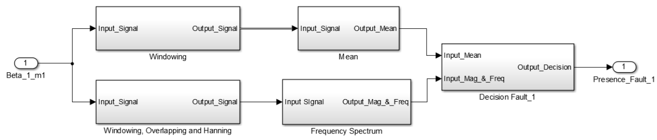

Fig. 7. The structure of the Simulink block which detects the presence of Fault_1.

Each detection method has its own block for windowing the input signal. The method based on the mean value needs sequences of 5 samples without overlapping which can be obtained using a *Zero-Order Hold* (to hold each sample value for one sample interval) and a *Buffer* (which groups every 5 sample values in a vector). The method based on frequency spectrum analysis needs sequences of 512 samples with 75% overlapping which can be obtained using as in the previous case, a *Zero-Order Hold* and a *Buffer* (having the size of 128 sample values). Moreover, three *Delay* blocks (determining 128, 256 and 384 sample periods delays respectively) are used, which keep the last three groups of 128 samples and together with the most recent group of 128 samples acquired are merged by the *Matrix Concatenate* block in order to obtain a sequence of 512 sample values which overlaps on 75% with the previous sequence. After this, a *Hanning* type window is applied on each sequence obtained. The signal's preparation for frequency spectral analysis is made in Simulink using the structure from Fig. 8.

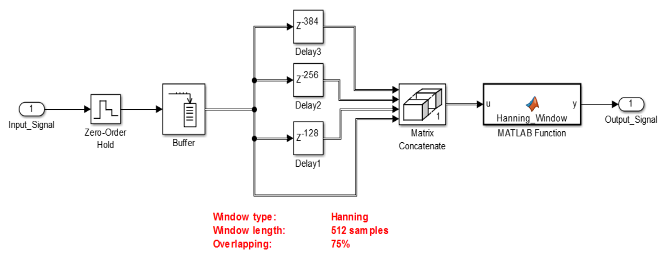

Fig. 8. The Simulink blocks for windowing, overlapping and application of Hanning type window operations used to detect the presence of Fault_1.

After windowing, the mean value and the frequency spectrum are determined using Matlab function blocks previously presented. The mean value, the magnitude and the frequencies of the spectrum (the last two are combined in a two column matrix) obtained are then send to the Decision block. This block applies the fault occurrence conditions described above using Matlab functions block. The results of each method (if the fault is present or not) are then send to a block which outputs the final decision (0 if the fault is absent, 2 if the fault is present and 1 if it the uncertainty state is present).

5.2. Gain factor faults in sensors

In the considered model of a wind turbine, two faults affect the sensors by modifying their outputs with a constant gain value. In this paper it will be considered only one of these faults:

- *Fault_5* – affects both the second sensor of the rotor's speed ($\omega_{r,m2}$) with the gain value 1.1 and the second sensor of the generator's speed ($\omega_{g,m2}$) with the gain value 0.9 in the time interval $[1000, 1100]\ s$ (Fig. 9)

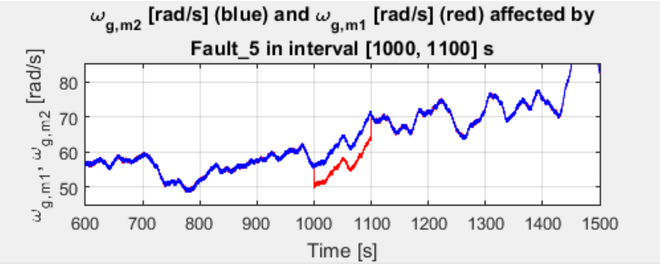

Fig. 9. Rotor's speed (ω_r) measured by the two redundant sensors: m1 (blue) affected by the Fault_5 in the time interval $[1000, 1100]\ s$ and m2 (red).

Similar to the case of the fixed value faults in sensors, this fault has a low severity, too. Even that the control loops are affected because the measurements become incorrect, due to the fact that physical redundancy is assured by using two sensors to measure the same physical phenomenon, its negative effects can be easily counteracted if it is detected on time.

The method used to detect this fault is based on the analysis of the auto-correlation of one of the affected signals. The definition formula of the auto-correlation of a signal contains the values of that signal (equation (10)). If the values of the signal increase (due to the presence of a fault which introduces a gain factor greater than 1), then the amplitude of the auto-correlation result will also increase and reversely, if the signal's values decrease, then the auto-correlation's amplitude will also decrease. Based on this observation, a fault which introduces a gain factor in a sensor's output can be detected by comparison with the auto-correlation's amplitude applied to the redundant sensors which measure the same physical phenomenon. If the maximum value of the difference between the auto-correlation's amplitude of the two redundant signals from a temporal window is greater than a threshold value (which has to be chosen such that the sensors' noise to not cause false detections), then the fault is present. Because the application of the auto-correlation function requires a sequence of values obtained from the sensors (having the length chosen such that useful information for detection process can be obtained in a time as short as possible), rectangular windows will be used for this method, too. The results by applying this method to the signals $\omega_{r,m2}$ and $\omega_{g,m1}$ and to their corresponding redundant signals are presented in Fig. 10 and Fig. 11. It can be observed that the values obtained from the signal ω_r (rotor's speed) when the fault is present are not higher than those obtained in normal operating conditions. In contrast, the values obtained from the signal ω_g (generator's speed) when the fault is present are clearly higher than the others. Thus, the detection method of this fault (*Fault_5*) will consider only the signal ω_g. A suitable method for the signal ω_r can be used and the results obtained to be combined, similar to the case of the fixed value faults described above, in order to obtain a higher certainty of the detection.

$$\Phi_{xx}(\tau) = \lim_{T\to\infty} \frac{1}{2T} \int_{-T}^{T} x(t) \cdot x(t+\tau) dt \qquad (10)$$

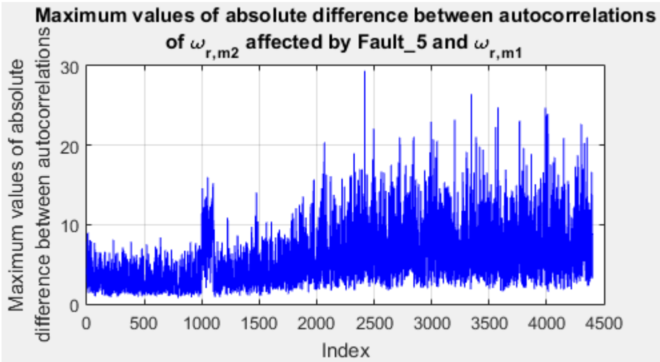

Fig. 10. The results obtained after computation of the maximum values of absolute difference between autocorrelations of redundant signals $\omega_{r,m2}$ (affected by Fault_5 in the time interval $[1000, 1100]\ s$) and $\omega_{r,m1}$. The values obtained when the fault is present are not higher than those obtained in the rest of the time.

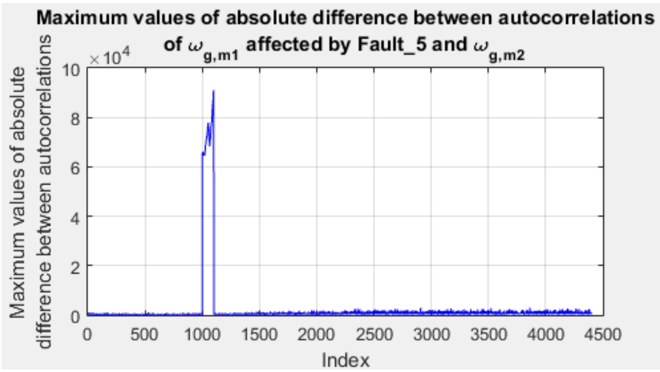

Fig. 11. The results obtained after computation of the maximum values of absolute difference between autocorrelations of redundant signals $\omega_{g,m1}$ (affected by Fault_5 in the time interval $[1000, 1100]\ s$) and $\omega_{g,m2}$. The values obtained when the fault is present are clearly greater than those obtained in the rest of the time.

The structure of the Simulink block which applies the presented method for detection of a gain factor fault (*Fault_5*) in a sensor is presented in Fig. 12. Both signals $\omega_{g,m1}$ and $\omega_{g,m2}$ are windowed in parallel using a *Buffer* of size 100. This size was chosen due to the best results obtained (only true detections of the fault obtained after a period of time (required for acquisition and processing) as short as possible) after several test. Further on, the auto-correlation is computed for each sequence and the results obtained are delivered to the next block which computes the absolute difference between them. The maximum value of this difference is then determined. Finally, the decision regarding the presence of gain value fault (*Fault_5*) (0 if the fault is absent, 2 if the fault is present) is taken in the *Decision_Fault_5* block. If the maximum value obtained is greater than a threshold value (which was chosen to be 3000 based on the results obtained after simulating the fault in different time moments) then the fault is present and the output signal of this detection block is modified to value 2. Otherwise, the output signal is maintained at value 0.

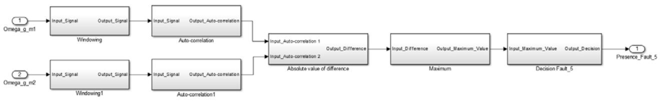

Fig. 12. The structure of the Simulink block which detects the presence of Fault_5 based on the signals $\omega_{g,m1}$ and $\omega_{g,m2}$.

As stated previously, a higher certainty in detection can be obtained by combining this method with a suitable one for signal ω_r and also indicating the presence of this fault only if in a consecutive number of time windows the fault is considered to be present (as it was done in the case of fixed value faults). This last technique has the disadvantage of introducing a big delay between the moments of occurrence and signaling of the fault (due to the fact that the time window used is long – 100 sample periods). In the performed tests, it was observed that this method was not necessary (no wrong alarms were made using the decisions of single time windows).

5.3. Offset value faults in actuators

In the considered model of a wind turbine, one fault affects an actuator by modifying its output with a constant offset value:

- *Fault_8* – affects the converter by adding a constant offset value ($100\ Nm$) to the generator's torque value (τ_g) in the time interval $[3800, 3900]\ s$ (Fig. 13).

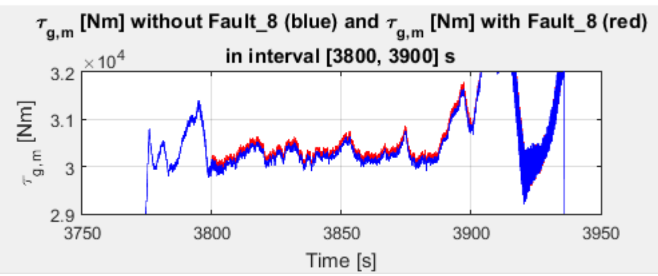

Fig. 13. Measured values of generator's torque (τ_g) when Fault_8 is not present (blue) and when it is present (red).

When the wind's speed is high enough in order to obtain the desired output electrical power, the controller starts to operate in the constant power production mode. Thus, the generator's torque is desired to remain constant by varying the pitch angles of the blades according to the wind's direction. When this type of fault occurs, the generator's torque is modified due to an offset in the converter's internal control loop. The severity of this fault is considered to be high because it determines a slow torque control which may lead in the worst case to damages to the wind turbine's mechanical structure.

The detection of this fault is based on the analytical model of the affected component. The dynamics of the converter used in the considered wind turbine model can be modelled as a first order system (equation (11)), where the constant design parameter α_{gc} is equal with 50 in this case (Odgaard, et al., 2009).

$$\frac{\tau_g(s)}{\tau_{g,r}(s)} = \frac{\alpha_{gc}}{s+\alpha_{gc}} \tag{11}$$

As stated in Section 4.1., a state-space estimator is required to be designed. Its dynamic has to be faster than the system's, so, based on the tests done, its Eigen value is chosen to be placed two times further away than the system's Eigen value (which is -50). Thus, by knowing that the estimator is a first order one and its Eigen value is equal with -100, the design is completed.

Also, due to the noise which affects the sensor from which the output of the analyzed component is taken, a low-pass Butterworth filter is required (Section 4.1). Based on the frequency spectrum of the residue signal obtained in this case (as the difference between the output of the converter modelled as a first order system and the output of the previous designed state-space estimator), the order of the filter is chosen to be 6 and the cut-off frequency $0.4\ Hz$. In Fig. 14 it is represented the obtained filtered residue. In the time interval when the fault occurs ($[3800, 3900]\ s$), higher values are obtained. Finally, a threshold value has to be chosen such that when the filtered residue is higher that this value, then the fault is signalized as being present.

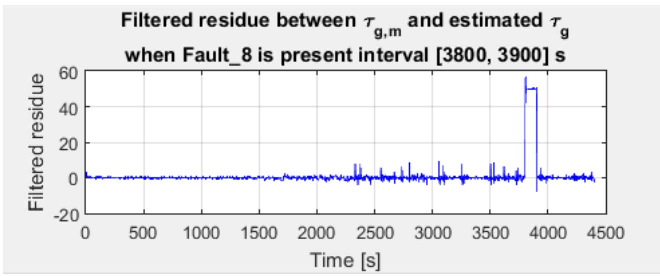

Fig. 14. The filtered residue between the measured generator's torque ($\tau_{g,m}$) and the estimated generator's torque using a state-space estimator.

The structure of the Simulink block which applies the described detection method is presented in Fig. 15. The state-space estimator is simulated using a State-Space block. Its inputs are $\tau_{g,r}$ and τ_g signals (which are the reference signal and the obtained generator's torque respectively) and its output is the estimated generator's torque. Then, the residue is computed and filtered using the designed Butterworth low-pass filter. The decision regarding the presence of the offset fault in converter *Fault_8* is taken in the last block, where the filtered residue values are compared with the threshold value $30\ Nm$ (determined after several tests). If the obtained values are greater than the threshold value, then the fault is present and the output signal of this detection block is modified to value 2. Otherwise, the output signal is maintained at value 0 (meaning that the fault is not present). As in the case of the previous fault, a robust detection can be achieved using a secondary detection method and combining the obtained results.

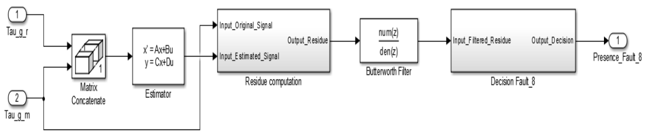

Fig. 15. The structure of the Simulink block which detects the presence of Fault_8 which affects the converter by introducing an offset value in the torque's value.

6. RESULTS AND DISCUSSIONS

The Simulink blocks for detecting the considered faults were constructed as presented before and placed in the wind turbine's benchmark model (Odgaard, et al., 2009) in order to function online.

During several tests, it was observed that all the faults were detected and no false detections were made. The average time differences between the occurrence and the detection moments and between the end of occurrence and the end of detection moments are presented in Table 1 and Table 2, respectively. Fig. 16 shows graphically the meaning of these time differences. In this figure, the signal obtained as output from the detection block has three values: 0 if the fault is absent, 2 if the fault is present and 1 if it the uncertainty state is present. Table 3 shows the detection coverage rate (percentage of the fault alarm duration with respect to the entire duration of the fault occurrence).

As stated previously, due to the fact that two detection methods were implemented and tested for the fixed value faults in sensors (*Fault_1*, *Fault_3* and *Fault_4*), an additional intermediary level of the output signal was added, which represents the uncertainty state. This state is activated when the fault detection conditions are met for one method but not for both. From the time differences presented in Table 1 and Table 2, it can be seen that when a fault occurs, the uncertainty state is activated after a short period (0.21 seconds on average), whereas the transition to the certain state takes on average 3 more seconds. This difference is caused by the length of the windows used in the processing methods (5 samples without overlapping for the mean detection method compared to 512 samples with an overlapping factor of 75% for the frequency-domain method). Shorter windows would lead to smaller time differences but would also cause false detections because less information would be used for analysis. Even though this fusion of two detection methods adds extra complexity to the solution and also adds an uncertainty state, the signalizing of a fault occurrence is more reliable. An odd number of detection methods could simplify the detection output by taking a majority vote among the decisions of the used methods.

For the detection of gain factor fault in sensors (*Fault_5*) and offset value faults in actuators (*Fault_8*) only one method was used and thus, the uncertain state is not used. This is the reason why Table 1 and Table 2 contain for these faults only the values corresponding to the time differences between the fault occurrence and the certain detection moments. It can be seen that *Fault_5* has the lowest values for time differences between the fault occurrence and the certain detection and between the end of fault occurrence and the end of certain detection, respectively, among all the considered faults. This is due to the small temporal window length (100 samples) used for the online detection. Even though *Fault_8* does not use any windowing, it has the highest time differences among all the analysed faults. The reason for this is given by the execution time needed for generating the prediction based on the analytical model, computing the residue and filtering it.

Overall, one can observe that the applied methods are able to promptly react to the considered fault occurrences. The used methods have the ability to detect the considered types of faults regardless of their parameters (i.e. gain factor and offset value) without any false detections. Thus, it can be said that the provided solution fulfils the requirements of robustness and reliability needed for any fault detection system.

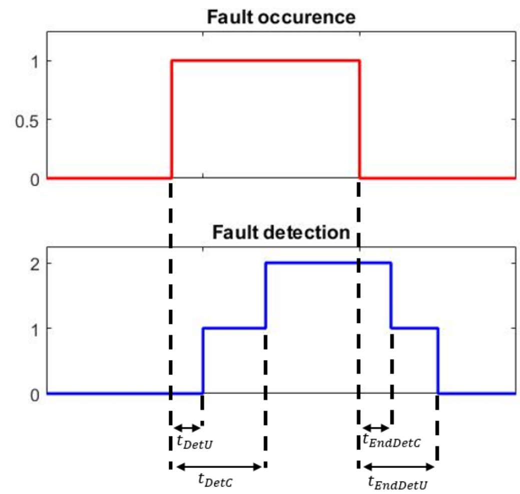

Fig. 16. The duration between the occurrence of a fault and its uncertain (t_{DetU}) and certain detection (t_{DetC}), respectively, and between the end of occurrence of a fault and the end of certain ($t_{EndDetC}$) and uncertain detection ($t_{EndDetU}$), respectively

Table 1. Time differences between the occurrence and the detection moments for each fault.

Fault	**Duration between the occurrence and the uncertain detection (t_{DetU}) [seconds]**	**Duration between the occurrence and the certain detection (t_{DetC}) [seconds]**
Fault_1	0.21	3.21
Fault_3	0.21	3.53
Fault_4	0.21	2.73
Fault_5	–	1.1
Fault_8	–	3.56

Table 2. Time differences between the end of occurrence and the end of detection moments for each fault.

Fault	Duration between the end of occurrence and the end of the uncertain detection ($t_{EndDetU}$) [seconds]	Duration between the end of occurrence and the end of certain detection ($t_{EndDetC}$) [seconds]
Fault_1	0.48	0.05
Fault_3	0.8	0.05
Fault_4	1.28	0.05
Fault_5	–	1
Fault_8	–	3.07

Table 3. Overlapping rate between the occurrence and the certain detection for each fault.

Fault	Overlapping rate between fault occurrence and certain fault detection [%]
Fault_1	96.79
Fault_3	96.47
Fault_4	97.27
Fault_5	98.9
Fault_8	96.44

As stated before, the first two steps of the fault diagnosis process are the detection and the isolation of the faults. The isolation implies finding the components affected by a certain fault. In the considered case of a wind turbine, this step is accomplished implicitly due to the fact that each fault affects a different signal and has a different signature. By knowing which signal has an abnormal behaviour, it can be said that the faults are isolated.

7. CONCLUSIONS

The worries regarding the increase of the global warming and the pollution level lead to an intense development of the electricity generation methods based on renewable resources (wind, sun, water, Earth's heat, hydrogen) in the last years (Tong, 2010). Even that the wind energy has some disadvantages (a high initial investment is necessary, the wind has a variable behaviour, the best positions for wind turbines are usually far from the place where electricity is needed), the advantages (no pollution is involved, worldwide availability, has the lowest price among all the other methods based on renewable resources) makes it the most promising energy source for the future (Wagner and Mathur, 2009).

The purpose of this paper was to present several fault detection and isolation methods for the case of a wind turbine. Due to the rapid growing of the wind turbines number, some of them being placed in positions very difficult to reach (offshore), the protection methods becomes very important. The methods studied in this paper can be divided into two categories: model-based methods (based on state-space estimators) and methods based on the wind turbine's signals analysis (in both frequency and time domains). For testing, a benchmark model of a real wind turbine implemented in Matlab and Simulink (Odgaard, et al., 2009) was used. The developed methods for detecting and isolating the faults which affect some of the sensors and the actuators of the wind turbine, were implemented as Simulink blocks and tested online. The obtained results are very good and prove that these methods can be used in a real case, implemented on an embedded system.

REFERENCES

ABB, 2011. Technical Application Papers No.13: Wind power plants. *Bergamo: ABB Sace*.

American Wind Energy Association, 2014. The Cost of Wind Energy in the U.S.. [Interactive] Available at: http://www.awea.org/Resources/Content.aspx?ItemNumber=5547 [Accessed 22 June 2016].

American Wind Energy Association, n.d. Wind Power Myths vs. Facts. [Online] Available at: http://www.pawindenergynow.org/wind/MythsvsFacts-FactSheet.pdf [Accessed 20 June 2016].

Blanke, M., Kinnaert, M., Lunze, J. and Staroswiecki, M., 2006. Diagnosis and Fault-Tolerant Control. *2nd ed. Berlin Heidelberg: Springer-Verlag*.

Burton, T., Sharpe, D., Jenkins, N. and Bossanyi, E., 2001. Wind Energy Handbook. *Chichester: John Wiley and Sons*.

Chiras, D., 2010. Wind Power - Basics. Gabriola Island: *New Society Publisher*.

Cooley, J. W. and Tukey, J. W., 1965. An Algorithm for the Machine Calculation of Complex Fourier Series. *Mathematics of Computation, 19(90)*, pp. 297-301.

Dahnoun, N., 2000. Digital Signal Processing Implementation Using the TMS320C6000 DSP Platform. *Boston: Prentice Hall*.

Esbensen, T. and Sloth, C., 2009. Fault Diagnosis and Fault-Tolerant Control of Wind Turbines, *s.l.: Thesis from Aalborg University*.

Gasch, R. and Twele, J., 2012. Wind Power Plants: Fundamentals, Design, Construction and Operation. *2nd ed. Berlin: Springer*.

Global Wind Energy Council, 2015. Global statistics. [Online] Available at: http://www.gwec.net/global-figures/graphs/ [Accessed 22 June 2016].

Hajiabady, S., Kerkyras, S., Hillmansen, S. and Tricoli, P., 2014. Efficient diagnostic condition monitoring for industrial wind turbines. *Renewable Power Generation Conference* (RPG 2014), pp. 1-5.

Hau, E., 2013. Wind Turbines: Fundamentals, Technologies, Applications, Economics. *3rd ed. Berlin: Springer*.

Katipamula, S. and Brambley, M. R., 2005. Methods for Fault Detection, Diagnostics, and Prognostics for Building Systems — A Review, Part I. *International Journal of HVACandR Research*, 11(1), pp. 3-25.

Khaligh, A. and Onar, O. G., 2010. Energy Harvesting - Solar, Wind, and Ocean Energy Conversion Systems. *Boca Raton: CRC Press*.

Lang, Z., 2014. "Digital Signal Processing" course. Sheffield: *University of Sheffield.*

Lee, Y. K., 2008. A Fauult Diagnosis Technique for Complex Systems Using Bayesian Data Analysis, s.l.: *Thesis from Georgia Institute of Technology.*

Luenberger, D., 1966. An Introduction to Observers. *IEEE Transactions on Automatic Control, Volume AC-11*, pp. 190-197.

Manwell, J., McGowan, J. and A.L., R., 2009. Wind energy explained: theory, design and application. *2nd ed. Chichester: John Wiley and Sons Ltd..*

Marcu, T. and Mirea, L., 2003. Diagnoza Anomaliilor Proceselor Tehnice. Iași: *Editura "Gh. Asachi".*

Mendes, M., Calado, J. and Sá da Costa, M., 2006. Fault Diagnosis System Based in Agents. *6th IFAC Symposium on Fault Detection, Supervision and Safety of Technical Processes*, 39(13), pp. 396-401.

Mukund, P. R., 1999. Wind and Solar Power Systems. *Boca Raton, Florida: CRC Press LLC.*

Odgaard, P. F. and Stoustrup, J., 2012. Results of a wind turbine FDI competition. 8th IFAC Symposium on Fault Detection, *Supervision and Safety of Technical Processes*, pp. 102-107.

Odgaard, P. F., Stoustrup, J. and Kinnaert, M., 2009. Fault Tolerant Control of Wind Turbines – a benchmark model. *Proceedings of the 7th IFAC Symposium on Fault Detection, Supervision and Safety of Technical Processes*, pp. 155-160.

Ozdemir, A. O., Seiler, P. and Balas, G. J., 2011. Wind Turbine Fault Detection Using Counter-Based Residual Thresholding. *Proceedings of IFAC world congress,* Volume 18, pp. 8289-8294.

Pollock, D. S. G., 1999. A Handbook of Time-Series Analysis, *Signal Processing and Dynamics. London: Academic Press.*

Poulsen, N. K. and Niemann, H., 2009. Active Fault Diagnosis - A Stochastic Approach. *7th IFAC Symposium on Fault Detection, Supervision and Safety of Technical Processes*, pp. 603-608.

Proakis, J. G. and Manolakis, D. G., 1996. Digital Signal Processing. *New Jersey: Prentice-Hall.*

Radisavljevic-Gajic, V., 2014. Linear Observers Design and Implementation. *Proceedings of 2014 Zone 1 Conference of the American Society for Engineering Education.*

Sathyajith, M., 2006. Wind Energy: Fundamentals, Resource Analysis and Economics. *Heidelberg: Springer.*

Tabatabaeipour, S. M., Odgaard, P. F. and Bak, T., 2012. Fault detection of a benchmark wind turbine using interval analysis. *American Control Conference* (ACC), pp. 4387-4392.

Tong, W., 2010. Wind Power Generation and Wind Turbine *Design. Billerica: WIT Press.*

Venkatasubramanian, V., Rengaswamy, R. and Yin, K. K. S., 2003. A review of process fault detection and diagnosis, *Part I: Quantitative model-based methods. Computers and Chemical Engineering*, 27(3), pp. 293-311.

Wagner, H.-J. and Mathur, J., 2009. Introduction to Wind Energy Systems: Basics,Technology and Operation. *Heidelberg: Springer.*

Wenxian, Y. and Tavner, P. W. M., 2008. Condition monitoring and fault diagnosis of a wind turbine with a synchronous generator using wavelet transforms. *4th IET Conference on Power Electronics, Machines and Drives,* pp. 6-10.

Wenxiu, L. and Fulei, C., 2010. Condition monitoring and fault diagnostics of wind turbines. *2010 Prognostics and System Health Management Conference,* pp. 1-11.